ISSN: 2414-1895 DOI: 10.6919/ICJE.202412_10(12).0006

Preparation and Performance Research of Coal Gangue-Slag Geopolymer Mortar

Mingjie Qin*

School of Materials Science and Engineering, Henan Polytechnic University, Jiaozuo 454000, Henan, China

*156301686@qq.com

Abstract

To achieve effective utilization of coal gangue, the effects of different slag contents on coal gangue-slag geopolymer mortar material (CSGM) were investigated. Results showed that for slag content at 40%, alkali equivalent at 7%, alkali solution modulus at 1.2 and water-cement ratio at 0.42, CSGM showed the highest compressive strength, which was 47.1 MPa. The increase in slag content caused an improvement in the compressive strength of CSGM, but a decrease in flexural strength. As the mineral powder content increases, the initial and final setting times of the sample are significantly shortened. The prepared CSGM has good resistance to sulfate attack. The higher slag content increased the formation of N-A-S-H and C-A-S-H gels, leading to a further refined microstructure and pore structure.

Keywords

Coal Gangue; Geopolymer; Sulfate Resistance; Pore Structure.

1. Introduction

Coal gangue is a solid waste discharged during coal mining, and it accounts for 1/10 to 1/4 of all coal mining by-products. China has a stockpile exceeding 7 billion tons[1, 2]. The accumulation, spontaneous combustion, and rainwater erosion of coal gangue pose serious threats to the surrounding soil, groundwater, and the living environment [3-6]. Therefore, it is urgent to accelerate the resource utilization of coal gangue.

Geopolymers are produced by the geopolymerization of aluminosilicate-rich mineralogies, such as metakaolin, slag, and fly ash, with alkali metal ion activators. It possesses high compressive strength [7, 8], good durability [9, 10], and chemical stability [11], as well as low energy consumption and reduced pollution levels [12, 13].Because the main chemical components of coal gangue are SiO_2 and Al_2O_3, and it contains a silicoaluminate structure, coal gangue may serve as a raw material for geopolymer. Existing research has shown that due to the low reactivity of coal gangue, geopolymer materials can be prepared from coal gangue only through thermal activation or by adding other highly reactive materials, such as slag [14-16]. Li [17]found that adding slag to the raw material, because of its high calcium content, helps improve the strength of the geopolymer. Huang et al. [18] found that the low active calcium content in coal gangue was the main reason for the low strength of geopolymers when using calcined coal gangue to prepare geopolymers. Ma et al.[19] observed that increasing the slag content led to a decrease in the geopolymer setting time and an increase in compressive strength. However, current research primarily focuses on geopolymers prepared from highly active materials such as calcined coal gangue, slag, metakaolin, and fly ash. There are few reports on the preparation of geopolymers using coal gangue as the main raw material.

ISSN: 2414-1895 DOI: 10.6919/ICJE.202412_10(12).0006

Therefore, in this study, coal gangue-slag geopolymer mortar material (CSGM) was prepared from coal gangue and slag, and sodium silicate and sodium hydroxide were used as alkali activators. The main purpose of this study was to determine the effect of varying slag content on the performance of CSGM and to propose a solution for the utilization of coal gangue. Through the Brunauer-Emmett-Teller (BET) and the scanning electron microscopy (SEM), the effect of different slag contents on the pore structure and microstructure of CSGM was determined.

2. Raw Materials and Test Methods

2.1 Raw Materials

Coal gangue: Coal gangue was obtained from Panzhihua (Sichuan, China). The main mineral components were quartz, clinochlore, and muscovite. The main chemical components were SiO_2 and Al_2O_3. The XRD results for determining the phase composition of the calcined coal gangue are shown in Figure 1.

S95 slag was obtained from Gongyi (Henan, China). Table 1 shows the main chemical composition of the raw material.

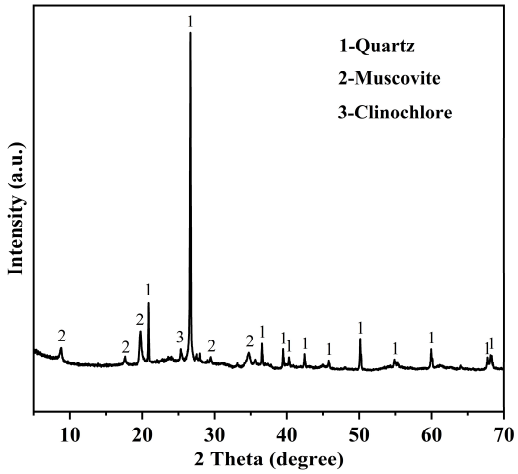

Figure 1. XRD patterns of calcined coal gangue

Table 1. Chemical compositions of raw material

Chemical composition	SiO_2	Al_2O_3	Fe_2O_3	K_2O	MgO	CaO	LOI
Calcined coal gangue	59.22	14.77	5.49	4.62	4.41	2.28	9.21
Slag	34.5	17.7	1.03	—	6.01	34.0	6.76

Alkali activator: Industrial grade Na_2SiO_3 (initial modulus ratio of SiO_2/Na_2O = 3.26, SiO_2 content of 26.98%, and Na_2O content of 8.53%) and NaOH (molecular weight of 40, purity ≥ 96%).

Standard sand was obtained from Xiamen (Fujian, China).

2.2 Experimental Design and Preparation

In this study, the raw materials included 60%-100% coal gangue, 0%-40% slag, and Na_2SiO_3 and NaOH as the alkaline activators. NaOH particles were mixed with Na_2SiO_3 and then cooled to room temperature to prepare an alkali solution with a modulus of 1.2. Each group of samples had a cement-sand ratio of 0.5 and a water-cement ratio of 0.42. Specific CSGM mixing ratios are shown in Table 2. The alkali solution modulus corresponds to the mass ratio of SiO_2/Na_2O in the activator solution.

The alkali equivalent is the ratio of the Na_2O content in the activator solution to the total mass of the raw materials [20]. According to the mix proportions of CSGM in Table 2, the raw materials and standard sand were placed in a mixer for dry mixing for 60 s. Then, the prepared alkali activator and

ISSN: 2414-1895 DOI: 10.6919/ICJE.202412_10(12).0006

water were added to the mixer together, with a mixing time of 120 s. Finally, the prepared mortar was poured into a mould of 40 mm×40 mm×160 mm. Following 1 day of curing under conditions of RH=95±1% and T=20±2 ℃, the specimen was demolded and transferred to the standard curing room to continue curing until the required ages (7 d and 28 d) and then tested. CSGMs maintained up to 28 days of age were immersed in a 5% Na_2SO_4 solution and water, respectively, for 28 days before being tested.

Table 2. Mixing proportions for CSGM

Specimen notation	Coal gangue /g	Slag/g	Alkali equivalent /%	Modulus	Water-cement ratio
K0	450	0	7	1.2	0.42
K1	405	45	7	1.2	0.42
K2	360	90	7	1.2	0.42
K3	315	135	7	1.2	0.42
K4	270	180	7	1.2	0.42

2.3 Test Method

The compressive strength and flexural strength of the CSGM were tested after curing for 7 and 28 days. For each curing time, three samples were selected and tested on a universal testing machine. The setting time of the CSGM was tested using a Vickers hardness tester. BET analysis was conducted using a TriStar II 3020 version 3.02 Physical Adsorption Meter to determine the pore size distribution of the CSGM. Adsorbent: N_2.

SEM (Merlin Compact) were used to characterize the microstructure of CSGM. E-beam accelerating voltage of 15 kV.

3. Results and Analysis

3.1 Setting Time

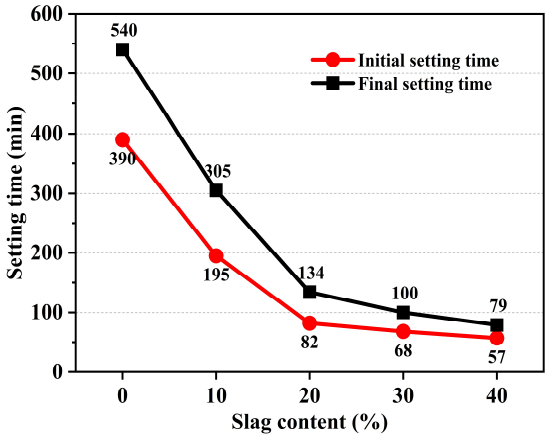

Figure 2. CSGM setting time with different slag contents

The effect of different slag contents on the setting time of CSGM is shown in Figure 2. As the slag content increased from 0% to 40%, both the initial and final setting times of the samples decreased continuously. The shortest initial setting time was 57 minutes, and the final setting time was 79 minutes, respectively, when the slag content reached 40%. Compared to the sample with 0% slag content, both the initial and final setting times of each sample were significantly reduced. This demonstrates that the slag content has a significant effect on the setting time of CSGM. This is because C-A-S-H gel (hydrated calcium silica-aluminate) forms more easily than N-A-S-H gel

ISSN: 2414-1895 DOI: 10.6919/ICJE.202412_10(12).0006

(hydrated sodium silica-aluminate) under alkaline conditions. Therefore, increasing the slag content raises the Ca^{2+} content. This leads to a faster generation of C-A-S-H gel, which in turn results in a faster setting time. The more C-A-S-H gel that is generated, the quicker the setting time becomes [21, 22].

3.2 Compressive and Flexural Strength

The influence of different slag contents on the compressive and flexural strength of CSGM is shown in Figure 3. As the slag content increases from 0% to 40%, the compressive strength shows an improving trend, but the flexural strength shows a decreasing trend. At a slag content of 40%, CSGM achieved its highest compressive strength, which was 42.4 MPa, and its lowest flexural strength was 3.55 MPa. Compared to specimens with 0% slag content, the 28-day compressive strength of the specimens increased by factors of 71%, 127%, 148%, and 159% for slag contents of 10%, 20%, 30%, and 40%, respectively. This indicates that the addition of slag is an effective method to improve the compressive strength of pure coal gangue geopolymer mortar. The 28-day flexural strength decreased in all samples, except for a slight increase with the addition of 10% slag (a 9.6% improvement). Especially at 30% and 40% slag content, the flexural strength decreased significantly, by 31.1% and 32.0%, respectively. The 28-day compressive strength did not increase significantly compared to the 7-day strength, indicating the early strength gain property of CSGM. This suggests that the geopolymerization reaction is largely completed during the early stage [23, 24].

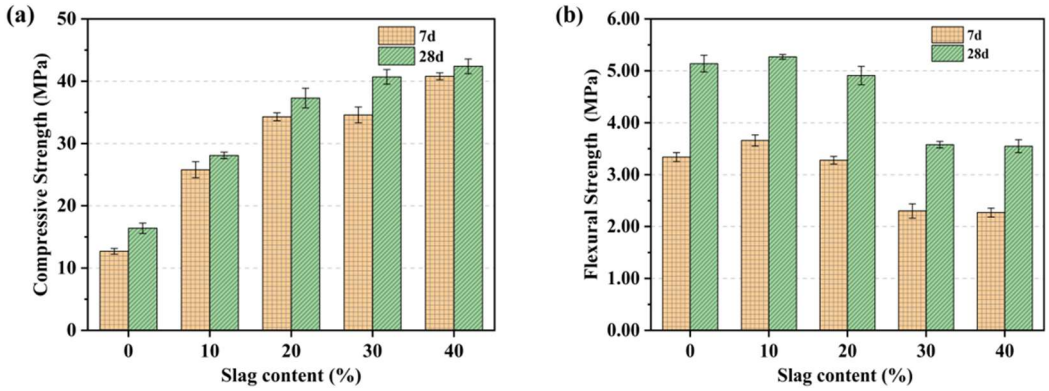

Figure 3. CSGM compressive and flexural strength with different slag contents (a) compressive strength, (b) flexural strength

3.3 Sulfate Resistance

Table 3. Sulfate resistance results of CSGM

Specimen notation	Influences	28 d Compressive strength /MPa	28 d Flexural strength /MPa
K0	Water	16.2	4.98
	Na_2SO_4 Solution	16.4	4.94
K1	Water	28.2	5.01
	Na_2SO_4 Solution	28.3	4.97
K2	Water	37.4	4.83
	Na_2SO_4 Solution	37.4	4.81
K3	Water	40.6	3.60
	Na_2SO_4 Solution	40.3	3.58
K4	Water	42.6	3.55
	Na_2SO_4 Solution	42.5	3.55

ISSN: 2414-1895 DOI: 10.6919/ICJE.202412_10(12).0006

The test results of the sulfate attack resistance of CSGM with different slag contents are shown in Table 3. After soaking in a 5% Na_2SO_4 solution, neither the compressive nor the flexural strength of the samples showed significant differences, except for a slight decrease in the compressive strength of samples K3 (30% slag content) and K4 (40% slag content); however, the rate of strength loss was not significant. This shows that by adding slag, CSGM still maintains good resistance to sulfate attack.

3.4 Pore Structure Analysis

The effects of the different slag contents on the pore size distribution within the CSGM are shown in Figure 4. Table 4 shows the pore structure parameters. As shown in Figure 4, the pore sizes of both groups of specimens were mainly distributed within the ranges of 50-100 nm, 20-50 nm, 5-20 nm, and 2-5 nm. The pore size distribution for both groups was essentially identical, showing a dominance of mesopores (2-50 nm), and both groups featured the presence of micropores (<2 nm). When the slag content increased from 20 to 40%, the large pores (>50 nm) decreased significantly, the peak pore size of the samples decreased gradually (from 34.7 nm to 23.4 nm), and the amount of pores of 2-20 nm increased with the increase of the slag content, and the total pore volume of the samples decreased gradually, and the specific surface area of the pores increased. This is because with the increase of slag content, the introduction of Ca^{2+} increased, so that the coal gangue involved in depolymerization and polaycondensation gradually increased, increasing the generation of hydration products N-A-S-H gel and C-A-S-H gel, the increase in the number of hydration products blocked the pore space, resulting in the structure of the specimen is more dense, and the lower porosity of the C-A-S-H gel can be better to fill the pore space, which reduces the porosity of the specimen [25], which in turn improves the strength of the sample.

Table 4. Pore structure parameters of CSGM

Samples	Cumulative pore volume /(cm^3/g)	Specific surface area of pores /(m^2/g)	Average pore size /nm
Slag-20%	0.054	12.672	15.904
Slag-40%	0.059	14.613	15.141

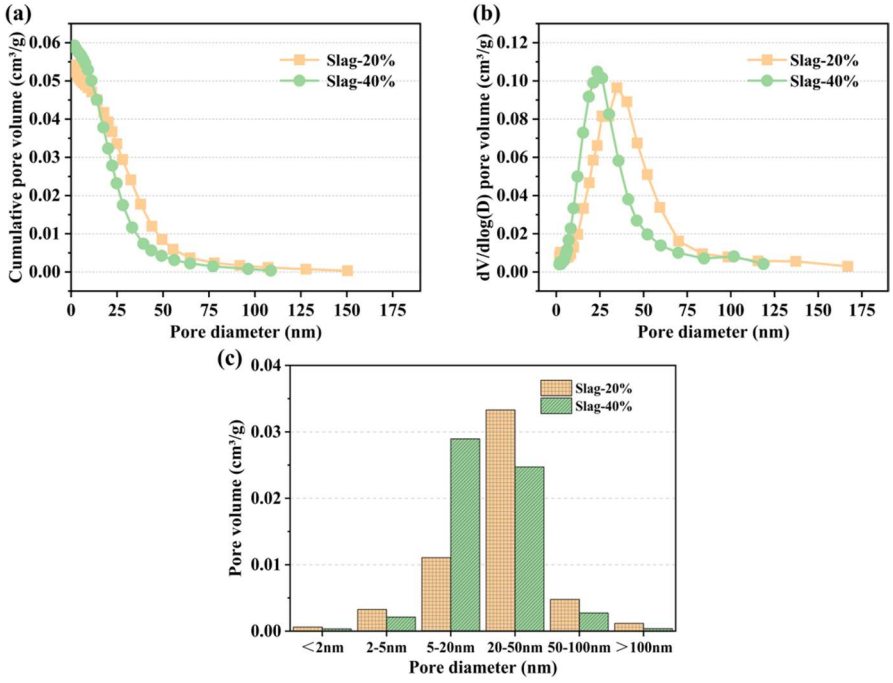

Figure 4. Pore structures of the CSGM (a) cumulative volume distribution curve, (b) pore size distribution curve, and (c) pore volume comparison plot

ISSN: 2414-1895 DOI: 10.6919/ICJE.202412_10(12).0006

3.5 SEM Analysis

An SEM image of CSGM after curing for 28 d is shown in Figure 5. CSGM contained many aluminosilicate gels and some unreacted coal gangue particles. Based on a comparison of the SEM images at 10 μm scale, the increase in slag content had a significant effect on the microstructure density of the samples. When the slag content was 0%, CSGM (K0) contained fewer gels, and unreacted coal gangue particles were visible on the surface of the sample. This indicates that the depolymerization and polycondensation of coal gangue in the samples are inadequate. As shown in Figure 5(b) to (d), with the increase of slag content, the number of gels in the CSGM gradually increases, the coverage area expands, and the overall structure becomes increasingly dense and homogeneous. Especially, Figure 5(d) shows that when the slag content is 40% (K4), the gel within the sample covers the largest area and appears in fragments, and the structure is the most dense, so this sample has the highest compressive strength. This is mainly because the addition of slag introduces a calcium source, and the $[SiO_4]^{4-}$ and $[AlO_4]^{5-}$ in the reaction system will combine with Ca^{2+} ions to form a C-A-S-H gel, and the higher the slag content, the more gel is generated in the sample, the microstructure becomes gradually denser, and ultimately, the compressive strength continues to improve [26].

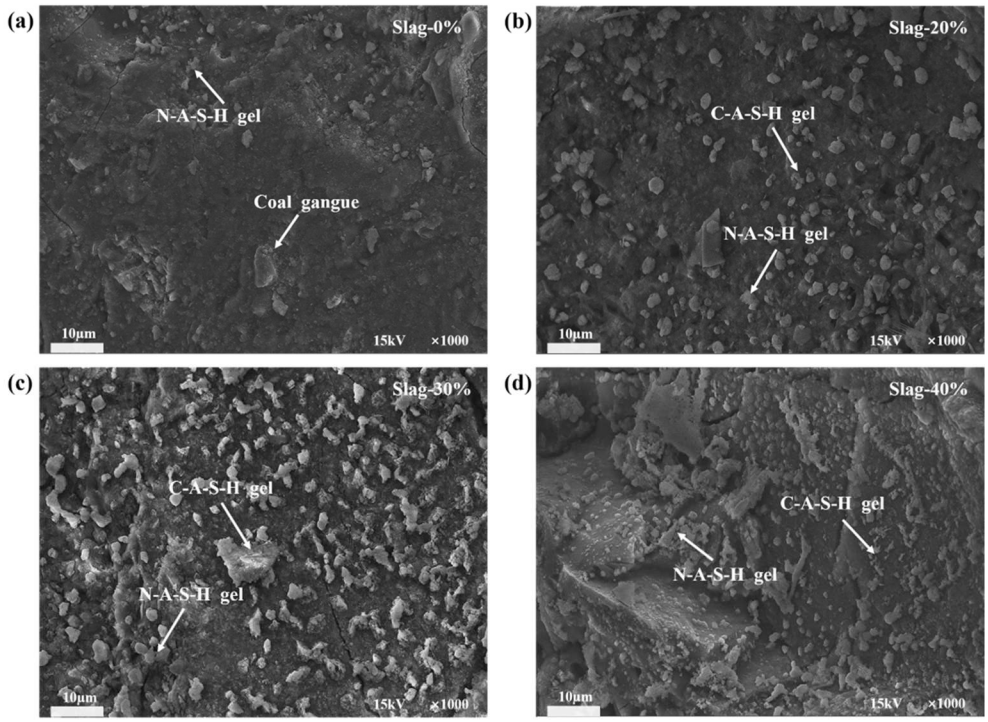

Figure 5. SEM images of the CSGM after curing for 28 d with (a) 0% slag content, (b) 20% slag content, (c) 30% slag content, (d) 40% slag content

4. Conclusion

When the slag content was 40%, the compressive strength of CSGM was the highest. An increase in the slag content decreased the flexural strength of CSGM, but was beneficial for increasing the compressive strength of CSGM. An increase in the slag content consistently improved the compressive strength of CSGM at each curing age.

The initial and final setting times of CSGM were significantly shortened by increasing the slag content from 0% to 40%, with a greater generation of C-A-S-H gel corresponding to a faster setting time. The prepared CSGM exhibits improved sulfate resistance.

The addition of slag optimized the pore structure of the samples. When the slag content increased from 20 to 40%, the large pores (>50 nm) decreased significantly. The peak pore size of the samples

ISSN: 2414-1895 DOI: 10.6919/ICJE.202412_10(12).0006

gradually decreased from 34.7 nm to 23.4 nm. As the slag content increased, the amount of pores in the 2-20 nm range also increased. The average pore size of the samples was gradually refined, the pore size distribution became more homogeneous, and the microstructure became denser.

Under the action of alkali activator, the increase of slag content promotes the condensation reaction between Ca^{2+} and silica-aluminate materials, which generates more C-A-S-H gels, thus enhancing the compressive strength of CSGM.

References

[1] Y. Fang, L. Yang, F. Rao, et al. Research progress on resource utilization of coal gangue by geological polymerization reaction, Min. Res. Dev. 43 (2023) 1–8.

[2] J. Chang, G. Du, J. Du, et al. Current situation of the comprehensive utilization of coal gangue in china and the related problems and recommendations, China Environ. Prot. Ind. (2022) 13–17.

[3] J. Li, J. Wang, Comprehensive utilization and environmental risks of coal gangue: a review, J. Clean. Prod. 239 (2019) 117946.

[4] C. Zhou, G. Liu, D. Wu, et al. Mobility behavior and environmental implications of trace elements associated with coal gangue: a case study at the Huainan Coalfield in China, Chemosphere 95 (2014) 193–199.

[5] Y.G. Liu, L.N. Yu, A.G. Zhou, Analysis of Coal Gangue Pollution Control Technology, 2nd International Conference on Advanced Materials and Engineering Materials (ICAMEM 2012), Trans Tech Publications Ltd, Beijing, PEOPLES R CHINA, 2012, pp. 941–944.

[6] L. Yang, J.F. Song, X. Bai, et al. Leaching behavior and potential environmental effects of trace elements in coal gangue of an open-cast coal mine area, Inner Mongolia, China, Minerals 6 (2) (2016) 18.

[7] D. Zurinskas, D. Vaiciukyniene, G. Stelmokaitis, et al. Clayey soil strength improvement by using alkali activated slag reinforcing, Minerals 10 (12) (2020) 12.

[8] F. Gu, J. Xie, C. Vuye, et al. Synthesis of geopolymer using alkaline activation of building-related construction and demolition wastes, J. Clean. Prod. 420 (2023) 138335.

[9] L.J. Kong, W.J. Zhao, D.X. Xuan, et al. Application potential of alkali-activated concrete for antimicrobial induced corrosion: a review, Construct. Build. Mater. 317 (2022) 13.

[10] T.A. Aiken, L. Gu, J. Kwasny, et al. Acid resistance of alkali-activated binders: a review of performance, mechanisms of deterioration and testing procedures, Construct. Build. Mater. 342 (2022) 22.

[11] B. Ren, J. Wang, Z. Zhou, et al. Regulation of the composition of metakaolin-based geopolymer: effect of zeolite crystal seeds, Case Stud. Constr. Mater. 19 (2023) e02421.

[12] H. Wu, C. Liang, D. Yang, et al. Development of sustainable geopolymer materials made with ground geopolymer waste powder as renewable binder up to 100, Constr. Build. Mater. 400 (2023) 132746.

[13] A. Zhou, K. Li, T. Liu, et al. Recycling and optimum utilization of engineering sediment waste into low-carbon geopolymer paste for sustainable infrastructure, J. Clean. Prod. 383 (2023) 135549.

[14] D. Yang, M.Y. Lu,D. Song, et al. Research Progress of Geopolymer Cement [J]. Materials Reports, 2021, 35(S1): 644-649.

[15] I. Ismail, S.A. Bernal, J.L. Provis, et al. Modification of phase evolution in alkali-activated blast furnace slag by the incorporation of fly ash[J]. Cement and Concrete Composites. 2014, 45: 125-135.

[16] Y. Li , Y. Yao , X. Liu , et al. Improvement on pozzolanic reactivity of coal gangue by integrated thermal and chemical activation [J]. Fuel, 2013, 109 527-533.

[17] L. Chao, H. Sun, L. Li, A review: The comparison between alkali-activated slag (Si+Ca) and metakaolin (Si+Al) cements, Cem. Concr. Res. 40 (9) (2010) 1341–1349.

[18] G. Huang, Y. Ji, J. Li, et al. Improving strength of calcinated coal gangue geopolymer mortars via increasing calcium content [J]. Construction and Building Materials, 2018, 166 760-768.

[19] H.Q. Ma, H.Y. Chen, H.G. Zhu, et al. Study on the drying shrinkage of alkali-activated coal gangue-slag mortar and its mechanisms, Construct. Build. Mater. 225 (2019) 204–213.

[20] Q.C. Song, Study on Preparation and Properties of Coal Gangue-based Geopolymer and Its Porousmaterials [D], Hengyang: University of South China, 2019:19-28.

ISSN: 2414-1895 DOI: 10.6919/ICJE.202412_10(12).0006

[21] García-Lodeiro I, Fernández-Jiménez A, Palomo A, et al. Effect of calcium additions on N–A–S–H cementitious gels[J]. Journal of the American Ceramic Society, 2010, 93(7): 1934-1940.

[22] Kramar S ,Šajna A ,Ducman V . Assessment of alkali activated mortars based on different precursors with regard to their suitability for concrete repair [J]. Construction and Building Materials, 2016, 124 937-944.

[23] Puligilla S ,Mondal P . Role of slag in microstructural development and hardening of fly ash-slag geopolymer [J]. Cement and Concrete Research, 2013, 43 70-80.

[24] J. Xie, J. Wang, R. Rao, et al. Effects of combined usage of GGBS and fly ash on workability and mechanical properties of alkali activated geopolymer concrete with recycled aggregate [J]. Composites Part B, 2019, 164 179-190.

[25] H.Q. Ma, Study on Performance of Alkali-activated Coal Gangue-slag Cementitious Materials and Durability of Concrete [D]. China University of Mining and Technology (beijing), 2021.

[26] F.D. Nurhayat, Utilization of Natural and Waste Pozzolans as an Alternative Resource of Geopolymer Mortar [J]. International Journal of Civil Engineering, 2018, 16 (2): 179-188.